Project Findings

There were six cloud interception events at the Whiteface site (July 4-5, 7, 16, 17, 20 and 22) occurring at different times of the day. The events lasted anywhere from two to twelve hours. Samples were collected hourly, except when the liquid water content was extremely high, in which case samples were collected every half-hour. At Davis there were also six fog events (December 18, January 4-5, 9, 10, 10-11 and 11-12) that generally began in the middle of the night and continued into mid-morning. There the liquid water content was generally rather low, so samples were collected either hourly or every two hours.

1. Drop composition and S(IV) oxidation in Whiteface Mountain, NY clouds

The chemical compositions of the samples collected at Whiteface Mountain were fairly homogeneous with respect to drop size. The cloudwater was found to be quite acidic, with pH values in the range 2.8 to 4.7. The pH values also appear to remain constant across the drop size spectrum (Fig. 1). This homogeneity is also characteristic of the other inorganic ions and aqueous H_2O_2. One to one scatter plots of samples collected using the sf-CASCC show that there is little difference between large and small drop concentrations for most ions (e.g. sulfate, Fig. 2). There does, however, exist some enhancement in the large drop fraction for the divalent cations. Additional samples collected using the CSU 5-stage cloud sampler reveal some size-dependence to drop composition that is not apparent with the two-stage collector data.

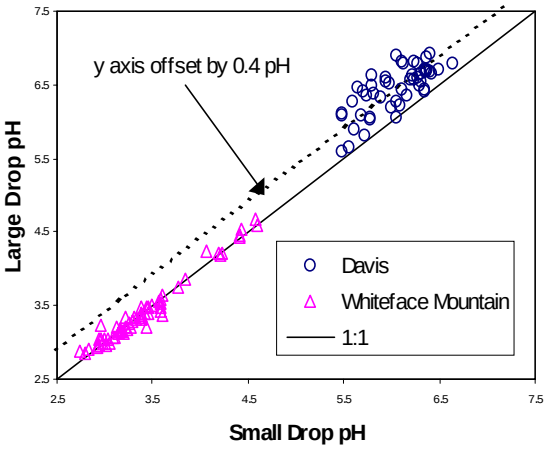

Figure 1. Comparison of pH in large and small drop sizes at Whiteface Mountain vs Davis.

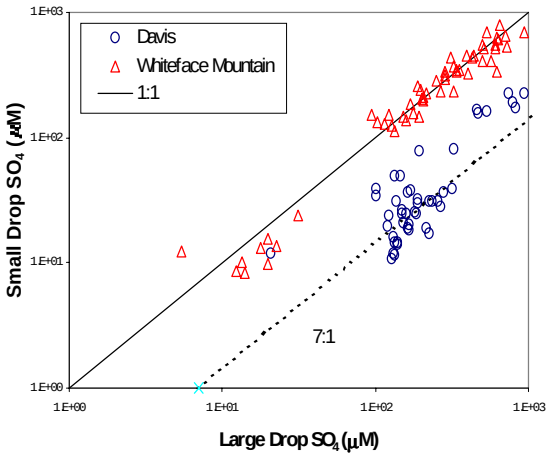

Figure 2. Comparison of sulfate in large and small drop sizes at Whiteface Mountain vs Davis.

Overall, however, the variation in drop composition as a function of drop size is smaller in these clouds than we have observed in most other situations we have studied. The oxidation rates calculated from the Whiteface Mountain cloud compositions suggest that indeed hydrogen peroxide is the dominant oxidant here. Also, as expected, the oxidation rates are nearly the same for both size fractions and the bulk samples. Ratios between the calculated rates in large and small drops, with some exceptions, are close to one.

The ratios of oxidation rates predicted in the large and small fog/cloud drop fractions were compared to ratios of sulfate produced in large and small fog/cloud drop fractions as determined using the tracer technique. The tracer technique compares ratios of sulfate/selenium in pre-fog or below-cloud aerosol with those in the fog/cloud water in order to determine the amount of sulfate produced in the fog/cloud. The results from Whiteface Mountain show that the amount of sulfate produced in the clouds is fairly uniform across the drop size spectrum. The ratio of in-cloud sulfate production between the large and small fractions is generally near one.

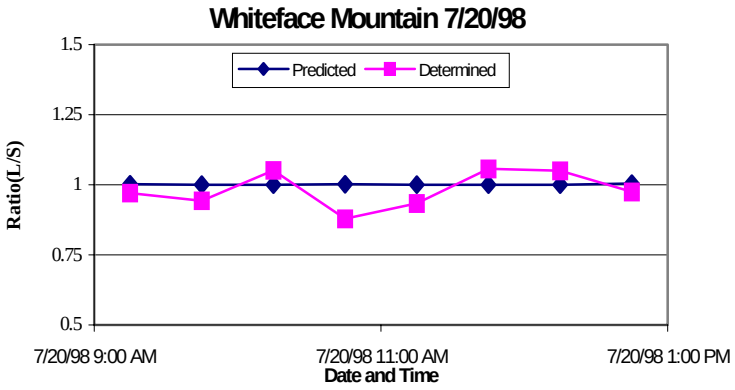

Figure 3. Comparison of predicted and tracer-determined large:small cloud drop S(IV) oxidation rate ratios for one of the studied cloud interception events.

The predicted S(IV) oxidation rate ratios for Whiteface Mountain match rather well with the tracer determined ratios of in-cloud sulfate production in large and small drops (see the example event highlighted in Figure 3). Both show large to small drop ratios near one, with no significant enhancement in either fraction. Therefore, Whiteface Mountain does indeed represent a good control case for this study, exhibiting the expected behavior.

2. Drop composition and S(IV) oxidation in Davis, California radiation fogs

The pH values of the Davis fog samples were high, consistent with past observations of Central Valley fog chemisty. Bulk fog pH values ranged from 5.3 to 6.8. A significant difference in pH values between the large and small fog drop samples was also observed, as seen in Figure 1. Large drop pH values were typically several tenths of a pH unit higher than small drop values.

Most of the measured inorganic ions show a strong trend towards higher concentrations in the small fog drop fraction. Figure 4 shows the observed size dependence for nitrate, sulfate, chloride and ammonium. Nitrate and ammonium ions are present at much higher concentrations than sulfate and chloride; however, it is clear that all four species are preferentially enriched in small fog drops. Concentrations of the divalent cations Ca^{2+} and Mg^{2+} were also found to be higher in the small drop fraction, a pattern that contrasts with many past observations of species size dependence at other locations. The concentration difference between large and small drop fractions for the divalent cations,

however, is not as strong as for the other ions. Concentrations of the trace metals Fe and Mn exhibit variable drop size dependence; in most sample periods they were enriched in small drops, but in some sample periods they showed little size dependence or were enriched in large drops.

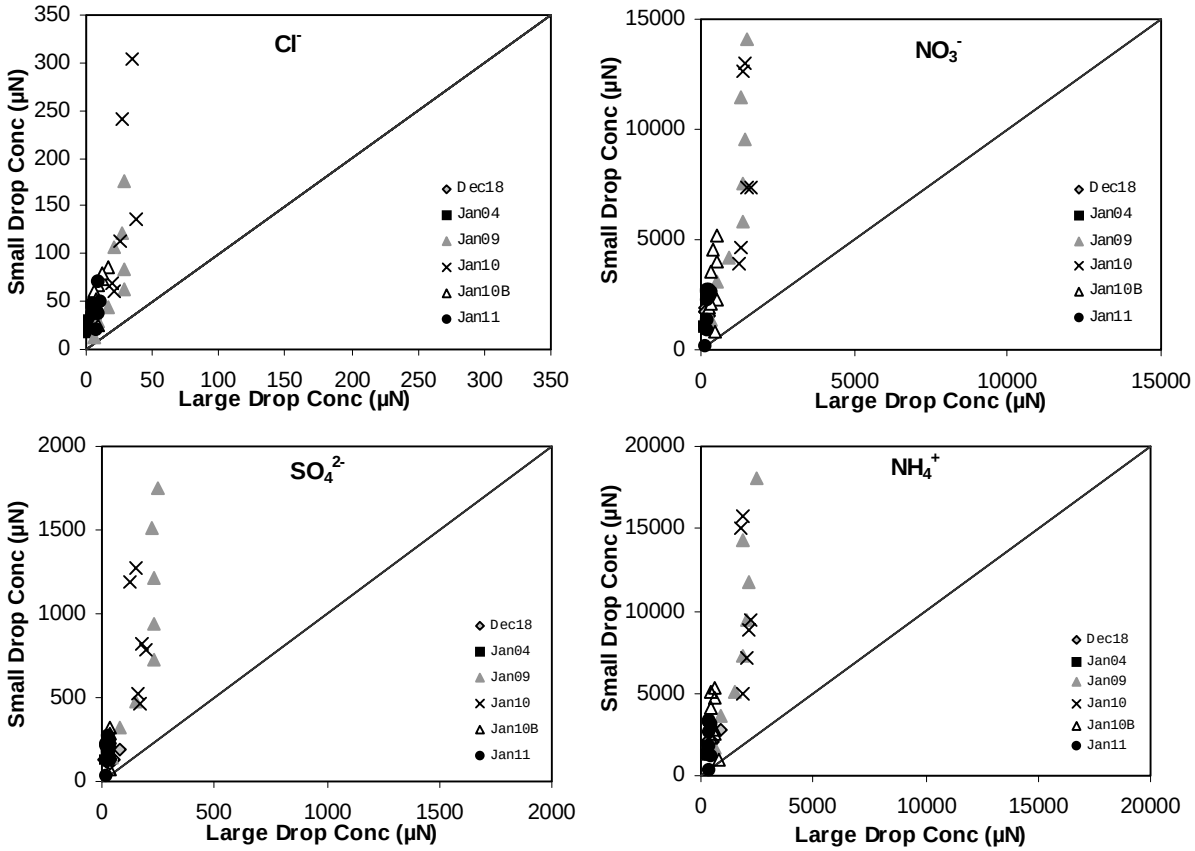

Figure 4. Fog drop size-dependence of chloride, nitrate, sulfate and ammonium concentrations in Davis, California radiation fogs.

In the fog drops there are two major sinks for S(IV), one is oxidation to form S(VI) and the other is complexation with HCHO to form hydroxymethanesulfonate (HMS). Aqueous S(IV) oxidation can occur via a number of different pathways. We consider three potentially important pathways here: oxidation by hydrogen peroxide, by ozone or autooxidation catalyzed by Fe(III) and Mn(II). Fog composition and trace gas concentration observations made during the study were used to initially evaluate potential rates of oxidation by each of these pathways. In this process we assumed Henry's law equilibrium was maintained between the gas and liquid phases, thereby neglecting potential rate limitations due to finite rates of mass transport and/or competing reactions. This initial analysis suggested that the ozone oxidation pathway was often dominant, with the hydrogen peroxide pathway also contributing significantly during some periods. The metal-catalyzed autooxidation pathway was found to be too slow to be an important contributor, even if the entire amounts of Fe and Mn measured in the fog drops were assumed to be present in catalytically active forms.

Results of this initial analysis indicate that S(IV) oxidation should occur much more rapidly in the large fog drops than in the small fog drops. This expectation results from the higher pH measured in large fog drops combined with faster S(IV) oxidation by ozone with increasing pH. Given the very rapid rate of oxidation expected at pH values above 6, the presence of abundant formaldehyde, and the large drop sizes present during the observed fog episodes, it is important to consider the potential for mass transport limitations and competing reactions to limit the aqueous phase S(IV) oxidation rates. Competition for aqueous S(IV) by formaldehyde and mass transport of several species were identified as likely factors that could strongly limit the rate of aqueous sulfate production under observed Davis fog conditions.

An aqueous drop chemistry model was utilized to calculate predicted rates of S(IV) depletion in the drops. The model, *AQCHEM*, calculates rates for the hydrogen peroxide and ozone S(IV) oxidation pathways and considers both gas phase and interfacial mass transport limitations. It was modified for this study by adding the S(IV)-formaldehyde reaction and including mass transport limitation in the aqueous phase. The *AQCHEM* model is a single drop model. In order to evaluate S(IV) reaction rates representative of those in the large and small drop fractions of the sf-CASCC, baseline simulations were run for drop diameters of 10 and 30 μm, with additional sensitivity analyses utilizing a range of drop sizes. Model inputs included measured fog compositions from the large and small drop sf-CASCC fractions, measured trace gas (sulfur dioxide, ozone, and hydrogen peroxide) concentrations, and temperature. Fog drop formaldehyde concentrations were estimated from available observations during the same fog episode in some periods when measurements were not available.

Figure 5 summarizes the model-predicted fate of S(IV) during the six fog episodes for the two baseline drop sizes (10 and 30 μm) chosen to represent the large and small fog drop sf-CASCC size fractions. The largest sink for S(IV), according to the model calculations, is its complexation with formaldehyde to form hydroxymethanesulfonate. This complexation reaction is predicted to account on average for 84% of the total S(IV) sink in both the large and small drop size fractions. This percentage, however, is probably somewhat over predicted, since the measured fog HCHO concentration input to the model simulation includes HMS as well as formaldehyde in its free and gem diol forms.

The model simulations suggest that oxidation of S(IV) accounts on average for approximately 16% of the total S(IV) sink in both drop size fractions. The contributions of the ozone and hydrogen peroxide oxidation pathways to aqeuous sulfate production differ with drop size, however. Simulations for the large fraction indicate that nearly 80% of the sulfate production for the larger drops is accomplished via the ozone oxidation pathway. The results for the small fraction, however, indicate the hydrogen peroxide oxidation pathway dominates the average sulfate production in the small drops. The overall dominance of the hydrogen peroxide pathway for small drop sulfate production results from several factors: typically lower pH values in the small drops,

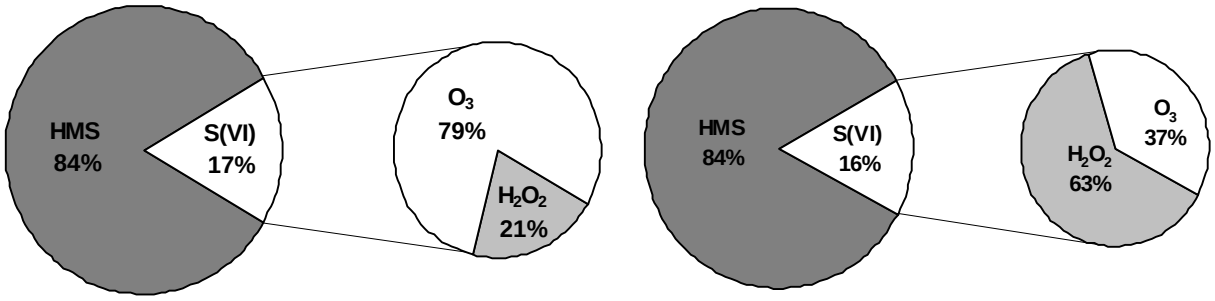

Figure 5. S(IV) sinks as calculated by the *AQCHEM* aqueous phase chemistry model for both the large (left figure) and small (right figure) drop fractions from the sf-CASCC.

high H_2O_2 concentrations during the first two fog events, and mass transport limitations to the rate of S(IV) oxidation by ozone during periods with higher pH.

Because most of the sampled fogwater was collected in the large drop fraction of the sf-CASCC, the overall fate of S(IV) in the Davis fogs should be very similar to the results depicted for the large drops. Volume weighted averages of the large and small drop fraction results suggest that overall complexation of S(IV) and HCHO to form HMS is the most important sink while the ozone oxidation pathway is responsible for approximately three-fourths of the total S(IV) oxidation.

The tracer technique was used to determine the amount of sulfate produced in the large and small fog drop size fractions collected with the sf-CASCC and in the CASCC2 bulk fog samples. The sulfate and selenium concentrations from the pre-fog aerosol measurements and the fog samples were used to obtain the concentration of sulfate produced by aqueous phase oxidation in each fog sample. In three cases (Jan 9, Jan 10B, and Jan 11) the ratio of sulfate to selenium observed in the fogwater was lower than that observed in the pre-fog aerosol, suggesting that the aerosol particles on which the fog drops formed differed in composition from the pre-fog aerosol. This may have occurred as a result of changes in aerosol composition at the site prior to the fog event or from entrainment of chemically different aerosol from above the boundary layer as the fog layer deepened. In these three episodes, the pre-fog aerosol sulfate to selenium ratio was replaced with the lowest bulk fog ratio of these species observed during each episode. An implicit assumption is made here that the bulk fog sample containing the lowest sulfate to selenium ratio had experienced little aqueous sulfate production. Since the amounts of aqueous sulfate production in these fogs was determined to be typically rather small (see Table 1, discussed below), possible error associated with this assumption should also be small.

Concentrations of sulfate produced in the fog, as determined by application of the tracer technique, are shown in Table 1. Also shown in Table 1 are ratios of sulfate determined to be produced *in situ* in large and small drop size fractions collected by the sf-CASCC. Application of the tracer technique of course has some uncertainty associated with it. The uncertainty is related to the percentage of total sulfate produced in the fog via a

power law equation; as the fraction of sulfate produced in the fog decreases the uncertainty goes up. Because the amount of sulfate produced in the fog is determined using the difference between aqueous and aerosol ratios of sulfate to selenium, the uncertainties can at times be very high. The uncertainty is estimated at 100% when the fraction of total sulfate produced in the fog drops is 14%; it decreases rapidly for higher fractions of *in situ* production.

Ratios of the amount of sulfate produced in the large fog drop fraction collected with the sf-CASCC to the amount produced in the small drop fraction are illustrated in Figure 6. Uncertainties, calculated as described above, are included as error bars. Only those sample periods for which aqueous formaldehyde concentrations were measured are included in the figure. Most of the tracer determined ratios fall between values of 0.1 and 1.0, indicating that the concentration of sulfate produced in small drops exceeded the concentration produced in large drops. Given the higher pH observed in the large drops, this observation suggests that the rate of S(IV) oxidation in the large drops was severely limited by an inability of reactants to be transported into the drop as fast as they were consumed by oxidation and reaction with formaldehyde.

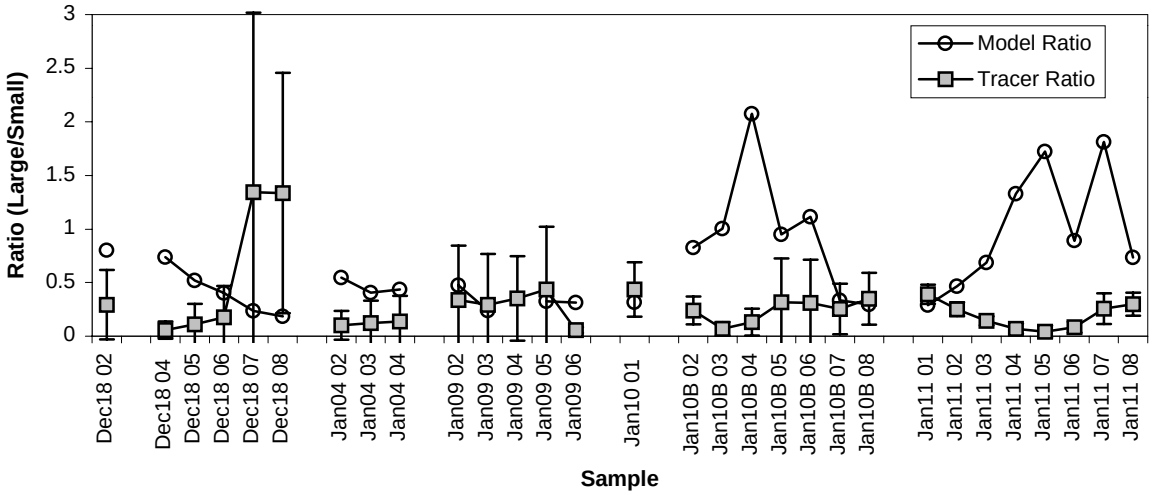

Figure 6. Comparison of tracer-determined ratios of sulfate produced by aqueous phase reaction in large and small drop size fractions with *AQCHEM* model-predicted large to small drop oxidation rate ratios. Uncertainty estimates are included on the tracer ratios as described in the text.

Figure 6 also depicts ratios of S(IV) oxidation rates predicted for the large and small drop fractions by the *AQCHEM* model simulations. Values of the predicted oxidation rate ratios also fall mainly between values of 0.1 and 1.0, indicating again that the HMS competition reaction and finite rates of reactant mass transport combine to greatly depress S(IV) oxidation rates in the large drops. In the absence of these factors, the large drop

oxidation rate is predicted to be several times faster than S(IV) oxidation in the small fog drops.

While it is possible to compare the tracer and model ratios plotted in Figure 6, this should be done cautiously. The tracer determined ratios reflect the amount of sulfate produced in the two drop size fractions over the lifetimes of the fog drops; the model ratios are based on predictions of instantaneous reaction rates made utilizing the average drop and gas phase composition measured during each individual fog sampling period. It is unreasonable to expect quantitative agreement between the ratios; qualitative agreement is expected if there is an accurate understanding of the processes determining aqueous phase sulfate production, the aqueous sulfate production rate exhibits a similar drop size-dependence over the duration of the fog episode, and the drop sizes chosen to represent the small and large drop fractions in the model simulations accurately reflect actual drop sizes collected by the two sf-CASCC sampling stages during each sampling period. The best agreement between the model and tracer ratios occurs for the third and fourth fog episodes, occurring during the mornings of January 9^{th} and 10^{th}. The fact that not all samples show close agreement is not surprising, as discussed above. In particular, the model-predicted large to small drop oxidation rate ratio is very sensitive to the choice of a representative large drop size. Increases in the modeled large drop size decrease the oxidation rate ratio significantly, providing closer agreement with the tracer ratios during many periods. The presence of very large drops in many of these fog episodes is supported by the relatively large amount of water collected on the first stage of the sf-CASCC, by large effective radii reported by the PVM, and by rapid water deposition velocities, determined from fog LWC and sedimentation flux rates measured at the site, characteristic of large fog drops. Sensitivity of the predicted rate ratio to changes in the ambient ozone concentration was also evaluated, as the low ozone concentrations measured during the fog periods were only a few parts per billion and were, therefore, considered relatively uncertain. Although small and large drop oxidation rates were individually sensitive to the assumed ozone concentration, their ratio was relatively insensitive.

3. SUMMARY

Application of the tracer technique to size-resolved fog and cloud drop samples collected at Whiteface Mountain, NY and Davis, CA revealed that S(IV) oxidation occurred at a rate independent of drop size in intercepted frontal/orographic clouds at Whiteface Mountain but varied with drop size in Davis radiation fogs. These findings were consistent with theoretical expectations.

Hydrogen peroxide is the dominant S(IV) oxidant in the acidic Whiteface Mountain clouds. Because hydrogen peroxide concentrations were independent of drop size, and the oxidation rate for this pathway is independent of pH in the relevant range, small and large drops are equally effective reservoirs for aqueous sulfate production.

Sinks for aqueous S(IV) in high pH Davis fog drops include oxidation by ozone or hydrogen peroxide and complexation by formaldehyde. Although oxidation by ozone

might be expected to be faster in the high pH large fog drops, mass transport limitations and rapid complexation of available S(IV) by formaldehyde combine to reduce S(IV) oxidation rates in the large drops below levels observed in more acidic small fog drops.

These studies demonstrate the applicability of the tracer technique to studies of drop size-dependent aqueous sulfate production. The technique should be considered for application to studies of sulfate production in other regions in the near future.

Table 1. Concentrations of sulfate (μ**M**) produced in the aqueous phase as determined using the tracer technique. Values are shown for bulk fog samples collected by the CASCC2 and for large and small fog drop size fractions collected by the sf-CASCC. Ratios of the large to small drop amounts are also included. n/a denotes the measurement is not available.

Sample	Bulk	Large	Small	Large/Small	Sample	Bulk	Large	Small	Large/Small
Dec18 01	n/a	17.3	n/a	n/a	Jan10 01	47.7	26.2	60.3	0.43
Dec18 02	3.5	3.7	12.7	0.29	Jan10 02	38.7	17.8	n/a	n/a
Dec18 03	1.5	1.7	8.7	0.20	Jan10 03	49.9	21.7	275.9	0.08
Dec18 04	1.1	0.6	11.4	0.06	Jan10 04	91.5	25.5	n/a	n/a
Dec18 05	1.5	0.9	8.0	0.11	Jan10 05	39.0	16.7	n/a	n/a
Dec18 06	1.6	1.2	7.1	0.17	Jan10 06	25.0	10.8	n/a	n/a
Dec18 07	7.2	8.2	6.1	1.34					
Dec18 08	16.6	14.6	10.9	1.34	Jan10B 01	11.8	6.8	n/a	n/a
Dec18 09	n/a	27.9	38.5	0.72	Jan10B 02	10.7	5.9	24.6	0.24
					Jan10B 03	4.6	2.6	37.2	0.07
Jan04 01	1.8	1.1	n/a	n/a	Jan10B 04	5.0	3.9	29.7	0.13
Jan04 02	2.0	1.3	12.9	0.10	Jan10B 05	4.0	5.3	16.8	0.32
Jan04 03	1.9	1.2	9.9	0.12	Jan10B 06	4.5	4.4	14.1	0.31
Jan04 04	2.2	1.3	9.2	0.14	Jan10B 07	3.6	3.1	12.4	0.25
Jan04 05	4.7	2.7	8.3	0.33	Jan10B 08	11.1	5.9	17.0	0.35
Jan04 06	5.1	2.7	8.6	0.32					
Jan04 07	4.4	1.5	19.9	0.08	Jan11 01	9.0	5.2	13.3	0.39
Jan04 08	6.3	4.4	23.9	0.18	Jan11 02	15.6	8.8	35.1	0.25
Jan04 09	7.1	5.3	35.2	0.15	Jan11 03	12.0	6.9	48.3	0.14
Jan04 10	8.1	5.9	31.5	0.19	Jan11 04	4.0	3.1	44.5	0.07
Jan04 11	7.2	5.4	23.1	0.24	Jan11 05	2.2	1.0	25.3	0.04
Jan04 12	7.5	6.0	30.7	0.19	Jan11 06	2.9	2.6	30.6	0.08
Jan04 13	9.6	6.1	26.9	0.23	Jan11 07	8.0	5.6	21.9	0.26
					Jan11 08	14.7	11.1	37.4	0.30
Jan09 01	5.1	2.9	8.7	0.34					
Jan09 02	10.4	6.6	19.5	0.34					
Jan09 03	16.7	9.3	31.8	0.29					
Jan09 04	26.6	20.6	58.4	0.35					
Jan09 05	30.7	24.5	56.4	0.43					
Jan09 06	40.4	29.8	535.0	0.06					
Jan09 07	35.1	32.6	n/a	n/a					
Jan09 08	52.6	20.7	n/a	n/a					